Transversely isotropic elastic properties of single-walled carbon nanotubes

Lianxi Shen and Jackie Li*
Mechanical Engineering Department, City College of New York, CUNY, 140th and Convent Avenue, New York, New York 10031, USA

(Received 21 August 2003; published 28 January 2004)

While it is known that the elastic properties of a single-walled carbon nanotube (SWNT) are transversely isotropic, the closed-form solutions for all five independent elastic moduli have not been solved completely. In this paper, an energy approach in the framework of molecular mechanics is used to evaluate the local and global deformations of a SWNT in a unified manner. This is carried out under four loading conditions: axial tension, torsional moment, in-plane biaxial tension, and in-plane pure shear, respectively, from which the closed-form expressions for the longitudinal Young's modulus, major Poisson's ratio, longitudinal shear, plane strain bulk, and in-plane shear moduli are obtained. It is shown that as the tube diameter increases, the major Poisson's ratio approaches a constant, the longitudinal Young's and shear moduli and the plane strain bulk modulus are inversely proportional to the tube diameter, and the in-plane shear modulus is inversely proportional to the third power of the tube diameter. The dependence of the elastic moduli of a SWNT on the tube diameter and helicity is displayed and discussed.

DOI: 10.1103/PhysRevB.69.045414 PACS number(s): 61.46.+w, 68.35.Gy, 62.20.Dc, 62.25.+g

I. INTRODUCTION

The single-walled carbon nanotubes (SWNT's) or multiwalled carbon nanotubes (MWNT's) are single or multiple layers of cylinder rolled up from graphene sheets.[1,2] It has been found that carbon nanotubes can possess exceptional mechanical properties.[3–10] For example, their axial Young's modulus could be as high as 1 TPa, their tensile strength may approach 100 GPa, and the deformation of an SWNT is completely reversible subjected to very large strains. The possible industrial applications of the nanotubes have stimulated experimental measurements and theoretical evaluations of the mechanical properties of SWNT's, MWNT's, and crystalline ropes of SWNT's.

The axial Young's modulus of SWNT's and MWNT's was experimentally measured using transmission electron microscopy (TEM) to observe the amplitude of the thermal vibrations of the anchored MWNT's or SWNT's.[11,12] It is reported that Young's modulus of MWNT's varies from 0.40 to 4.15 TPa with an average of 1.8 TPa (Ref. 11) and that of SWNT's is in the range from 0.90 to 1.70 TPa with an average value of 1.25 TPa (Ref. 12). The axial Young's modulus of MWNT's, nanoropes of SWNT's, and SWNT's was also probed using the tip of an atomic force microscope (AFM) to bend the anchored MWNT's and simultaneously record the force displacement relationship.[5,13–14] The reported values are 0.69 to 1.87 TPa with an average of 1.28 TPa for MWNT's,[5] 0.81 TPa for nanoropes of SWNT's,[13] and 1.2 TPa for SWNT's.[14] Some other experimental results of the axial Young's modulus are 1 TPa for MWNT's,[15] 2.8–3.6 TPa for SWNT's, 1.7–2.4 TPa for MWNT's,[6] and 0.22–0.68 for MWNT's.[16] The technical difficulty makes the experimental determination of other elastic moduli, such as Poisson's ratio and bulk and shear moduli, a rather challenging task.

The elastic moduli of SWNT's and MWNT's were theoretically studied using atomistic models, including the molecular dynamics based on empirical potentials,[17–27] the tight-binding-based approaches,[28–32] and the first principles of quantum mechanics.[33–35] It is noticed that a large variation of Young's modulus was obtained in these calculations—say, 0.76 TPa (Ref. 35), 0.97 TPa (Ref. 21), 1 TPa (Ref. 24), 1.26 TPa (Ref. 13), and 1.5 TPa (Ref. 18). A few continuum mechanics models were also proposed, in which a carbon nanotube is modeled as a thin shell of cylinder[19,36–38] or a beam.[39] Essentially, these continuum models are based on the effective concept, which can be very successful for some specific purposes if the effective elastic properties are properly determined. Another model that is located between the continuum mechanics and molecular mechanics is the structure mechanics model, in which a carbon nanotube is modeled as many truss members[40] or many beam members.[41] The sectional property parameters of the truss or beam members are obtained by correlating the structure mechanics and molecular mechanics. For these structure mechanics models, the involved number of nodes is the same as that of atoms. So different from the continuum mechanics models, the structure mechanics models cannot effectively save the effort of computational simulation compared with the direct molecular mechanics approach. Besides, a homogenization method for the atomic or molecular system was proposed,[25] which incorporates interatomic potentials into a continuum analysis.

It is noticed that most of the existing theoretical models for the elastic moduli of SWNT's or MWNT's are numerical ones, and these numerical calculations are mainly focused on the axial Young's and shear moduli and the major Poisson's ratio. To our knowledge, the plane strain bulk and in-plane shear moduli associated with the in-plane biaxial tensile and pure shear loading conditions have not been reported. Furthermore, the only closed-form expressions, which were recently derived using force equilibrium analysis in the framework of molecular mechanics, are for the axial Young's modulus and major Poisson's ratio.[26]

In this study, an energy approach in the framework of molecular mechanics is proposed. Compared with the force

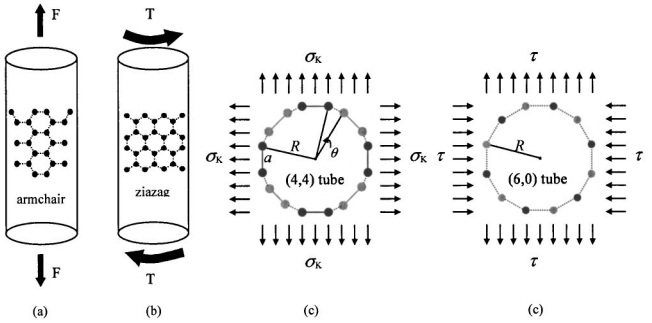

FIG. 1. The four types of loading conditions: (a) for axial tension, (b) for torsional moment, (c) for in-plane bi-axial tension, and (d) for in-plane pure shear.

equilibrium analysis,[26] the energy approach avoids the effort to visualize the molecular system of a SWNT to the effective stick-spiral system and can give instant insight into the local and global deformations of a SWNT. So the relatively complicated cases of the deformations of a SWNT subjected to the loading conditions of the torsional moment and in-plane pure shear stresses can be similarly solved. As a result, a set of closed-form expressions for the deformations and five independent elastic moduli of a SWNT are obtained.

II. ELASTIC MODULI OF A SWNT

The Young's modulus, Poisson's ratio, and shear modulus of a SWNT have been theoretically studied mainly in a numerical manner. The three moduli are here denoted as E_{11}, ν_{12}, and G_{12} by taking direction 1 as the axial direction along the tube. It is known that the three moduli are defined by imaging the SWNT as a thin shell of cylinder. When the global deformations of the SWNT are concerned or when it is effectively thought as a solid cylinder, the effective elastic properties of a SWNT are transversely isotropic. Therefore, five independent moduli are needed to completely describe the transversely isotropic elastic behavior. In this paper, the five independent effective elastic moduli are taken as the longitudinal Young's modulus, major Poisson's ratio, longitudinal shear modulus, and plane-strain bulk and in-plane shear moduli, which are denoted as $\overline{E}_{11}$, $\overline{\nu}_{12}$, $\overline{G}_{12}$, $\overline{K}_{23}$, and $\overline{G}_{23}$, respectively. The overbar indicates the effective properties of a SWNT. To our knowledge, these five moduli have not been completely solved. To extract the five moduli, four loading conditions, i.e., axial tension for $\overline{E}_{11}$ and $\overline{\nu}_{12}$, torsional moment for $\overline{G}_{12}$, in-plane biaxial tension for $\overline{K}_{23}$, and in-plane pure shear for $\overline{G}_{23}$, are applied to the SWNT, respectively. Schematic figures for these four loading conditions are shown in Figs. 1(a)–1(d). For the cases of (c) and (d) in Fig. 1, two ends of the SWNT are constrained so that the length of the tube stays unchanged which satisfies the plane-strain condition. An energy approach in the framework of molecular mechanics is developed to derive a set of closed-form expressions of the local and global deformations of the SWNT under these four loading conditions. Once the deformations are obtained, the elastic moduli including E_{11}, ν_{12}, and G_{12} and $\overline{E}_{11}$, $\overline{\nu}_{12}$, $\overline{G}_{12}$, $\overline{K}_{23}$, and $\overline{G}_{23}$ can be immediately extracted according to the corresponding definitions.

A. Longitudinal Young's modulus and major Poisson's ratio

According to the molecular mechanics that is based on the concept of molecular force field,[42] the total molecular potential energy U of a molecular system can be expressed as a sum of several individual energy terms,

$$U = U_\rho + U_\theta + U_\omega + U_\tau + U_{vdw} + U_{es}, \tag{1}$$

where U_ρ, U_θ, U_ω, and U_τ are the energies associated with bond stretching, angle variation, inversion, and torsion, and U_{vdw} and U_{es} denote the energies associated with van der Waals and electrostatic interactions. Various functional forms may be used to describe these energy terms.

For a SWNT subjected to an axial loading at small strain, as shown in Fig. 1(a), it is assumed that only the two energy terms associated with bond stretching and angle variation in Eq. (1) are significant in the total molecular potential energy, and other terms such as inversion, torsion, and van der Waals and electrostatic interactions may be negligible. Furthermore, due to the small deformations and the atomic interactions near the equilibrium structure, the total molecular potential energy U of a SWNT is expressed as a sum of simple harmonic potentials as follows:

$$U = \frac{1}{2}\sum_i C_{\rho,i}(\mathrm{d}b_i)^2 + \frac{1}{2}\sum_j C_{\theta,j}(\mathrm{d}\theta_j)^2, \tag{2}$$

where $\mathrm{d}b_i$ and $\mathrm{d}\theta_j$ are the elongation of bond i and the variation of bond angle j, and $C_{\rho,i}$ and $C_{\theta,j}$ are the force constants associated with the ith bond stretching and jth angle variation. The parameters for the force constants and equilibrium structure may be obtained by fitting a set of experimental data or quantum mechanics calculations. In the study, the properties of graphite are taken as reference point to get the force constants.

Since the local deformations around all the atoms are similar due to the symmetry of atomic structure and axial loading, a representative atom and a representative segment of SWNT with length l can be used for the energy analysis. So the total system potential energy of the segment of SWNT can be expressed as

$$\Pi = U - W = NU_0 - F\mathrm{d}l, \tag{3}$$

where W is the virtual work of the axial loading force F, N is the atom number of the segment of SWNT, and $\mathrm{d}l$ and U_0 are the global elongation of the segment of SWNT and the potential energy of the representative atom. The principle of minimum potential energy is written as

$$\delta\Pi = \delta(U - W) = 0. \tag{4}$$

So if U_0 and $\mathrm{d}l$ are expressed through some independent variables characterizing the local deformations around the atom, the principle can give a set of linear equations for these unknown independent variables.

For a (n,n) armchair SWNT subjected to an axial tensile force F, Fig. 2(a) shows the three chemical bonds a, b, and b,

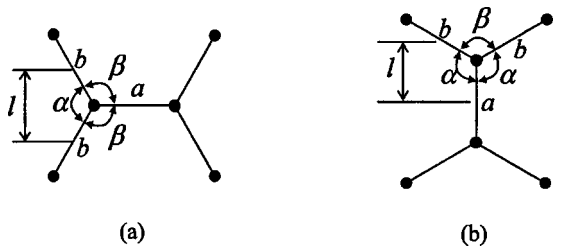

FIG. 2. Bonds and bond angles around a representative atom and a representative segment of a SWNT with the length l: (a) for a (n,n) nanotube and (b) for a $(n,0)$ nanotube.

three bond angles α, β, and β associated with the representative atom, and the length l of a representative segment of SWNT. The atom number in the representative segment of SWNT is $2n$. The geometrical relationship of (n,n) nanotube can be obtained as

$$\cos\beta+\cos\phi\cos\frac{\alpha}{2}=0, \tag{5}$$

where the angle between the bond a and the plane b-b is ϕ with $\phi=\pi/(2n)$, which is the rotation angle of the bond a around the symmetry axis of the SWNT with the plane b-b being reference. As the relationship (5) always holds and the angle ϕ keeps unchanged for the axial loading condition, differentiating Eq. (5) leads to

$$\mathrm{d}\beta=-\frac{\sin\frac{\alpha}{2}}{2\sin\beta}\cos\phi\,\mathrm{d}\alpha. \tag{6}$$

Thus, the independent variables may be chosen as $\mathrm{d}\alpha$, $\mathrm{d}a$, and $\mathrm{d}b$ in the possible variables $\mathrm{d}\alpha$, $\mathrm{d}\beta$, $\mathrm{d}a$, and $\mathrm{d}b$ characterizing the local deformations. The segment length l and the perimeter of the tube S can be expressed as

$$l=b\sin\frac{\alpha}{2} \tag{7}$$

and

$$S=2n\left(a+b\cos\frac{\alpha}{2}\right). \tag{8}$$

Similarly, differentiating both sides of Eqs. (7) and (8) leads to the relationships of the global and local deformations as follows:

$$\mathrm{d}l=\sin\frac{\alpha}{2}\mathrm{d}b+\frac{1}{2}b\cos\frac{\alpha}{2}\mathrm{d}\alpha \tag{9}$$

and

$$\mathrm{d}S=2n\left(\mathrm{d}a+\mathrm{d}b\cos\frac{\alpha}{2}-\frac{1}{2}b\sin\frac{\alpha}{2}\mathrm{d}\alpha\right). \tag{10}$$

The bond a and b are shared by two atoms. So the potential energy U_0 can be given as

$$U_0=\frac{1}{4}C_\rho\mathrm{d}a^2+\frac{1}{2}C_\rho\mathrm{d}b^2+\frac{1}{2}C_\theta\eta_1\mathrm{d}\alpha^2 \tag{11}$$

with

$$\eta_1=1+\frac{1}{2}\sin^2\frac{\alpha}{2}\cos^2\phi/\sin^2\beta. \tag{12}$$

Therefore, the total system potential energy Π in Eq. (3) becomes

$$\Pi=2n\left[\frac{1}{4}C_\rho\mathrm{d}a^2+\frac{1}{2}C_\rho\mathrm{d}b^2+\frac{1}{2}C_\theta\eta_1\mathrm{d}\alpha^2\right]-F\left(\sin\frac{\alpha}{2}\mathrm{d}b+\frac{1}{2}b\cos\frac{\alpha}{2}\mathrm{d}\alpha\right). \tag{13}$$

Based on Eq. (4), the independent variables $\mathrm{d}\alpha$, $\mathrm{d}a$, and $\mathrm{d}b$ can be solved as

$$\mathrm{d}a=0, \tag{14}$$

$$\mathrm{d}b=\frac{F}{2nC_\rho}\sin\frac{\alpha}{2}, \tag{15}$$

$$\mathrm{d}\alpha=\frac{F}{4nC_\theta\eta_1}b\cos\frac{\alpha}{2}. \tag{16}$$

Therefore, the axial strain $\varepsilon_{11}=\mathrm{d}l/l$ and the circumferential strain $\varepsilon_{22}=\mathrm{d}S/S$ can be obtained as

$$\varepsilon_{11}=\frac{F}{2nbC_\rho}\sin\frac{\alpha}{2}\left(1+\frac{1}{4\eta_1}b^2\cot^2\frac{\alpha}{2}\right) \tag{17}$$

and

$$\varepsilon_{22}=\frac{F\sin\alpha}{4nC_\rho\left(a+b\cos\frac{\alpha}{2}\right)}\left(1-\frac{b^2C_\rho}{4C_\theta\eta_1}\right). \tag{18}$$

As the relative change of the tube radius R is the same as that of the perimeter, i.e., $\mathrm{d}R/R=\mathrm{d}S/S$, ε_{22} also represents the radial strain of the tube.

By imagining the nanotube as a thin shell of cylinder with radius R and thickness t or a solid cylinder with radius R, the longitudinal Young's modulus of the SWNT E_{11} or $\bar{E}_{11}$ can be defined as

$$E_{11}=\frac{F}{2\pi Rt\varepsilon_{11}}\quad\text{or}\quad\bar{E}_{11}=\frac{F}{\pi R^2\varepsilon_{11}}. \tag{19}$$

The modulus based on the definition associated with a solid cylinder is also called the effective modulus of the SWNT, which is indicated by an overbar. And the definition of the major Poisson's ratio of the SWNT does not require a thickness, which can be defined as

$$\nu_{12}=-\frac{\varepsilon_{22}}{\varepsilon_{11}}. \tag{20}$$

So it is seen from the definition based on a thin shell of cylinder that the Young's modulus is dependent of the thickness t. In fact, different values of the thickness have been suggested to define the Young's modulus.[19,39] Another definition that is independent of the thickness has been proposed by the second derivative of the strain energy with respect to the axial strain per unit area of the nanotube[29] which is also referred to as the surface Young's modulus.[26] The surface Young's modulus, denoted as E_{11}^s here, is actually the ratio of the axial force per length over the perimeter and the axial strain, i.e., $E_{11}^s=(F/(2\pi R))/\varepsilon_{11}$. The relationships between the Young's moduli based on various definitions can be written as follows:

$$E_{11}=E_{11}^s/t \quad \text{and} \quad \overline{E}_{11}=E_{11}^s/(R/2). \tag{21}$$

Using Eqs. (17)–(21), the surface Young's modulus E_{11}^s and major Poisson's ratio can be obtained as

$$E_{11}^s=\frac{C_\rho}{\sin(\alpha/2)[1+\cos(\alpha/2)][(C_\rho a^2/C_\theta)\cot^2(\alpha/2)/(4\eta_1)+1]}, \tag{22}$$

$$\nu_{12}=\frac{\cos(\alpha/2)[(C_\rho a^2/C_\theta)/(4\eta_1)-1]}{[1+\cos(\alpha/2)][(C_\rho a^2/C_\theta)\cot^2(\alpha/2)/(4\eta_1)+1]}. \tag{23}$$

The parameters of the equilibrium structure of the undeformed SWNT are taken as $a=b=0.142$ nm, $\alpha\approx 2\pi/3$, and $\beta\approx\pi-\arccos[(1/2)\cos(\pi/2n)]$ (Ref. 43). So Eqs. (22) and (23) can be further reduced as

$$E_{11}^s=\frac{4\sqrt{3}C_\rho}{3(C_\rho a^2/C_\theta)/(4\eta_1)+9}, \tag{24}$$

$$\nu_{12}=\frac{(C_\rho a^2/C_\theta)/(4\eta_1)-1}{(C_\rho a^2/C_\theta)/(4\eta_1)+3}. \tag{25}$$

For a $(n,0)$ zigzag SWNT, Fig. 2(b) shows the three chemical bonds a, b, and b and three bond angles α, β, and β, associated with a representative atom, and the length l of a representative segment of SWNT. The atom number in the representative segment of SWNT is n. The angle between the bond a and the plane b-b is ϕ with $\phi=\pi/n$. Similar geometrical relationships to Eqs. (5)–(8) can be derived as follows:

$$\cos\beta+\sin^2\alpha\cos\phi-\cos^2\alpha=0, \tag{26}$$

$$\mathrm{d}\beta=\frac{\sin(2\alpha)}{\sin\beta}(1+\cos\phi)\mathrm{d}\alpha, \tag{27}$$

$$l=\frac{1}{2}(b-a\cos\alpha), \tag{28}$$

$$S=2na\sin\alpha. \tag{29}$$

By taking the independent variables as $\mathrm{d}\alpha$, $\mathrm{d}a$, and $\mathrm{d}b$, the total system potential energy Π becomes

$$\Pi=n\left[\frac{1}{4}C_\rho\mathrm{d}a^2+\frac{1}{2}C_\rho\mathrm{d}b^2+C_\theta\eta_2\mathrm{d}\alpha^2\right]-F\left[\frac{1}{2}(\mathrm{d}b-\cos\alpha\mathrm{d}a+a\sin\alpha\mathrm{d}\alpha)\right], \tag{30}$$

with

$$\eta_2=1+\frac{1}{2}\frac{\sin^2(2\alpha)}{\sin^2\beta}(1+\cos\phi)^2. \tag{31}$$

The similar derivations to the case of (n,n) SWNT lead to

$$E_{11}^s=\frac{(1-\cos\alpha)C_\rho}{\sin\alpha[2+\cos^2\alpha+(C_\rho a^2/C_\theta)\sin^2\alpha/(2\eta_2)]}, \tag{32}$$

$$\nu_{12}=\frac{\cos\alpha(1-\cos\alpha)[1-(C_\rho a^2/C_\theta)/(2\eta_2)]}{2+\cos^2\alpha+(C_\rho a^2/C_\theta)\sin^2\alpha/(2\eta_2)}. \tag{33}$$

Using $a=b$, $\alpha\approx 2\pi/3$, and $\beta\approx\arccos[1/4-(3/4)\cos(\pi/n)]$ (Ref. 42), Eqs. (32) and (33) can be further reduced as

$$E_{11}^s=\frac{4\sqrt{3}C_\rho}{3(C_\rho a^2/C_\theta)/(2\eta_2)+9}, \tag{34}$$

$$\nu_{12}=\frac{(C_\rho a^2/C_\theta)/(2\eta_2)-1}{(C_\rho a^2/C_\theta)/(2\eta_2)+3}. \tag{35}$$

It is noticed that Chang and Gao[26] have derived the closed-form expressions using force equilibrium approach to analyze a SWNT subjected to an axial tensile loading in the same framework of molecular mechanics. To derive the equilibrium equations, they visualized a SWNT as an effective ''stick-spiral'' system, in which an elastic stick and a spiral spring are used to model the force and twisting moment resulting from the C—C bond stretching and angle variations. Also, the stick is assumed to have an infinite bending stiffness because the chemical bond always remains straight. It is expected that the present results should be agreeable with those of Chang and Gao.[26] However, for the case of $(n,0)$ SWNT, the results from the two approaches do not coincide. The parameters $1/(4\eta_1)$ and $1/(2\eta_2)$ in Eqs. (24) and (25) for the (n,n) armchair tube and in Eqs. (34) and (35) for the $(n,0)$ zigzag tube can be simplified to

$$1/(4\eta_1)=\frac{7-\cos(\pi/n)}{32+2\cos(\pi/n)}, \tag{36}$$

$$1/(2\eta_2)=\frac{5+2\cos(\pi/n)-3\cos^2(\pi/n)}{14+12\cos(\pi/n)-2\cos^2(\pi/n)}. \tag{37}$$

The corresponding parameters in the similar expressions by Chang and Gao[26] are

$$\lambda=\frac{7-\cos(\pi/n)}{32+2\cos(\pi/n)} \quad \text{for the } (n,n) \text{ tube} \tag{38}$$

and

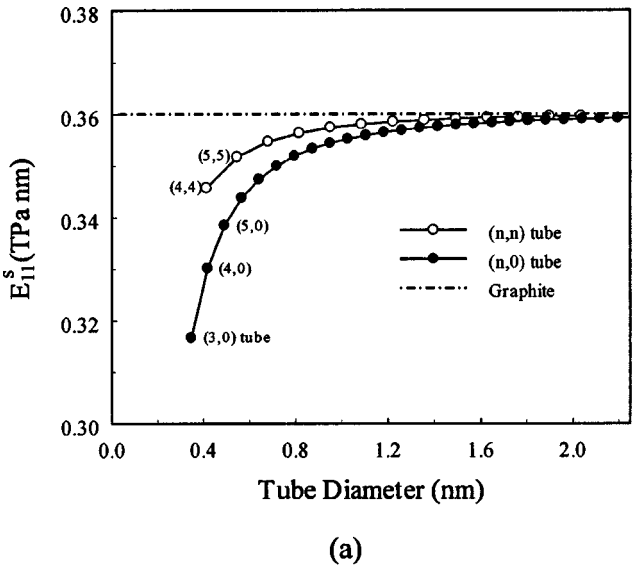

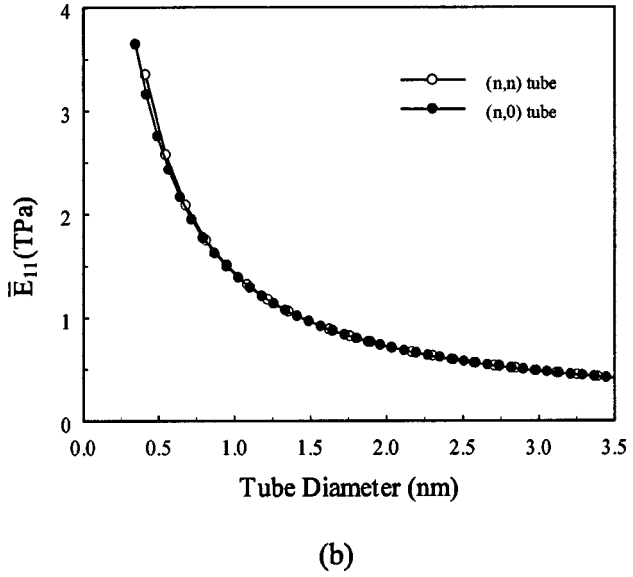

FIG. 3. Variation of the longitudinal Young's modulus with the tube diameter: (a) for the surface longitudinal Young's modulus and (b) for the effective longitudinal Young's modulus.

$$\lambda = \frac{5-3\cos(\pi/n)}{14-2\cos(\pi/n)} \quad \text{for the } (n,0) \text{ tube.} \tag{39}$$

Equations (37) and (39) do not coincide even though their difference is small.

Let the values predicted by Eqs. (24) and (25) equal to those of graphite, i.e., 0.36 TPa nm and 0.16 for the limiting case of $n\to\infty$; the force constants can be obtained, i.e., $C_\rho = 742$ nN/nm and $C_\theta = 1.42$ nN nm. Then, based on Eqs. (24), (25), (34), and (35), Figs. 3(a) and 3(b) plot the results of the surface Young's modulus and the effective Young's modulus, and Fig. 4 is for the major Poisson's ratio. It is seen from Figs. 3(a) and 4 that the surface Young's modulus and Poisson's ratio are close to those of graphite when the tube diameter is larger than 1 nm. The comparison of the surface

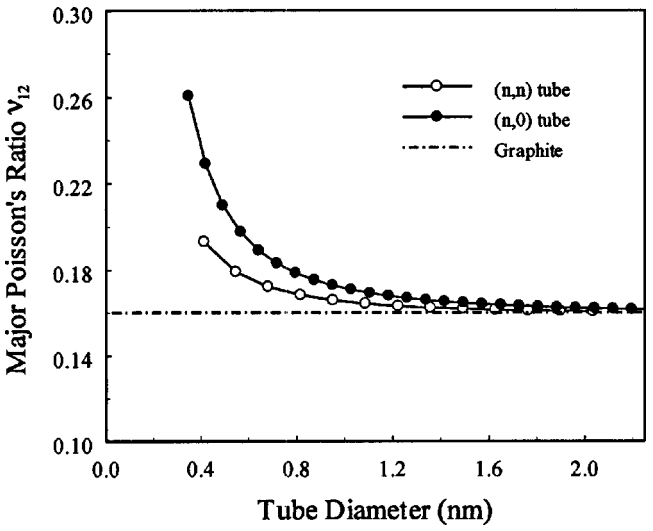

FIG. 4. Variation of the major Poisson's ratio with the tube diameter.

Young's modulus with other numerical results[24,31] has been given and discussed,[26] which is not repeated here.

B. Longitudinal shear modulus

The longitudinal shear modulus of a hollow or solid cylinder is the only property which is relevant to the torsion angle per unit length of the cylinder subjected to a torque. So based on the analysis of a SWNT subjected to a torque T, as shown in Fig. 1(b), the longitudinal shear modulus of the SWNT can be extracted. The geometrical analysis for the local deformation of a SWNT subjected to a torque is much more complicated than that associated with axial loading. So some details are depicted.

For a (n,n) armchair SWNT, it is assumed that the atoms always keep on the cylindrical surface of the SWNT when they deform under the torque. Based on the symmetrical analysis, the local deformation can be determined using two generalized displacements, i.e., ds and $d\varphi$ as shown in Fig. 5(a). So the three bond stretching, i.e., da, db_1, and db_2, and the three angle variations $d\alpha$, $d\beta_1$, and $d\beta_2$ around a typical atom can be solved as

$$da = 0, \quad db_2 = -db_1 = B_\varphi d\varphi + B_a ds, \tag{40}$$

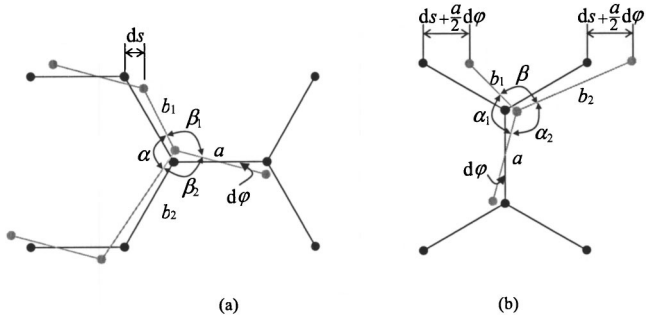

FIG. 5. Two generalized displacements ds and $d\varphi$ characterizing the bond stretching and angle variations around a representative atom: (a) for a (n,n) nanotube and (b) for a $(n,0)$ nanotube.

with

$$B_\varphi = a\sin(\alpha/2) \quad \text{and} \quad B_s = (R/a)\sin\theta, \tag{41}$$

$$\mathrm{d}\alpha = 0, \quad \mathrm{d}\beta_2 = -\mathrm{d}\beta_1 = A_\varphi \mathrm{d}\varphi + A_s \mathrm{d}s, \tag{42}$$

with

$$A_\varphi = \sin(\alpha/2)(1-\cos\beta)/\sin\beta \tag{43}$$

and

$$A_s = R[\sin\theta(1+\cos(\alpha/2)\cos\phi) - \sin(2\phi)]/(a^2\sin\beta), \tag{44}$$

where the angle θ is shown in Fig. 1(c), and the higher-order quantities of ds and dφ have been ignored in the above derivations. The virtual work of the torque T is $W = T\mathrm{d}S/R$. So the total system potential energy Π can be written as

$$\Pi = 2n\left(\frac{1}{2}C_\rho \mathrm{d}b^2 + C_\theta \mathrm{d}\beta^2\right) - T\mathrm{d}S/R. \tag{45}$$

Based on the principle $\delta\Pi = \delta(U-W) = 0$, the unknown generalized displacements ds and dφ can be solved. Then, the torsional angle per unit length of the SWNT, i.e., θ_0 with $\theta_0 = ds/(Rl)$, can be obtained as

$$\theta_0 = \frac{T}{2n\sin(\alpha/2)aR^2}[A_\varphi^2/C_\rho + B_\varphi^2/(2C_\theta)]/(A_\varphi B_s - A_s B_\varphi)^2. \tag{46}$$

Similarly, by imagining the nanotube as a thin shell of cylinder with radius R and thickness t or a solid cylinder with radius R, the two longitudinal shear moduli of the SWNT, denoted as G_{12} or $\overline{G}_{12}$, respectively, can be defined as follows:

$$G_{12} = \frac{T}{2\pi t R^3 \theta_0} \quad \text{or} \quad \overline{G}_{12} = \frac{T}{\pi R^4 \theta_0}, \tag{47}$$

where the torsional angle formula of the thin shell of cylinder or a solid cylinder subjected to a torque has actually been used. The surface longitudinal shear modulus with the relationship $G_{12}^s = tG_{12}$ or $G_{12}^s = (R/2)\overline{G}_{12}$ can be extracted from Eq. (46) as follows:

$$G_{12}^s = \frac{\sqrt{3}}{3}(A_\varphi B_s - A_s B_\varphi)^2/[A_\varphi^2/C_\rho + B_\varphi^2/(2C_\theta)]. \tag{48}$$

Using $R/a = 3n/2\pi$, $\alpha = 2\pi/3$, $\cos\beta = -\frac{1}{2}\cos\phi$, and $\phi = \pi/2n$, the above expression can be further reduced as

$$G_{12}^s = \frac{6\sqrt{3}n^2}{\pi^2} \times \frac{\sin^2(\pi/n)}{2[2+\cos(\pi/2n)]^2 + [4-\cos^2(\pi/2n)](C_\rho a^2/C_\theta)}. \tag{49}$$

For a $(n,0)$ zigzag SWNT, the local deformation can also be determined using two generalized displacements, i.e., ds and dφ as shown in Fig. 5(b). Similarly, the three bond stretching, i.e., da, db_1, and db_2, and the three angle variations dβ, dα_1, and dα_2 around the representative atom can be solved as follows:

$$\mathrm{d}a = 0, \quad \mathrm{d}b_1 = -\mathrm{d}b_2 = B_\varphi \mathrm{d}\varphi + B_a \mathrm{d}s, \tag{50}$$

with

$$B_\varphi = \frac{1}{2}R\sin(\phi/2), \quad B_s = -\frac{R}{a}\sin(\phi/2), \tag{51}$$

$$\mathrm{d}\beta = 0, \quad \mathrm{d}\alpha_1 = -\mathrm{d}\alpha_2 = A_\varphi \mathrm{d}\varphi + A_s \mathrm{d}s, \tag{52}$$

with

$$A_\varphi = \frac{R}{a}\frac{\sin(\phi/2)}{\sin\alpha}\left(1 - \frac{1}{2}\cos\alpha\right), \quad A_s = -\frac{R}{a^2}\cot\alpha\sin(\phi/2). \tag{53}$$

The system potential energy Π can be written as

$$\Pi = n\left(\frac{1}{2}C_\rho \mathrm{d}b^2 + C_\theta \mathrm{d}\alpha^2\right) - T(\mathrm{d}s/2 + a\mathrm{d}\varphi/4)/R. \tag{54}$$

Based on the principle, i.e., $\delta\Pi = \delta(U-W) = 0$, the unknown generalized displacements ds and dφ can be solved. Then, the torsional angle per unit length of the SWNT, i.e., θ_0 with $\theta_0 = (\mathrm{d}s/2 + a\mathrm{d}\varphi/4)/(Rl)$, can be obtained as

$$\theta_0 = \frac{T}{n(1-\cos\alpha)aR^2}\left[\left(A_\varphi - \frac{a}{2}A_s\right)^2 \Big/ C_\rho + \left(B_\varphi - \frac{a}{2}B_s\right)^2 \Big/ (2C_\theta)\right] \Big/ (A_\varphi B_s - A_s B_\varphi)^2. \tag{55}$$

And the surface longitudinal shear modulus can be obtained as

$$G_{12}^s = 4\sqrt{3}(A_\varphi B_s - A_s B_\varphi)^2/[(A_\varphi^2 - a^2A_s^2)/C_\rho + (B_\varphi^2 - a^2B_s^2)/(2C_\theta)]. \tag{56}$$

Using $R/a = \sqrt{3}n/2\pi$, $\alpha = 2\pi/3$, and $\phi = \pi/n$, the above expression can be further reduced as

$$G_{12}^s = \frac{8\sqrt{3}n^2\sin^2(\pi/2n)C\rho}{\pi^2(6 + C_\rho a^2/C_\theta)}. \tag{57}$$

The variation of the surface longitudinal shear modulus G_{12}^s with the diameter is plotted in Fig. 6(a), and Fig. 6(b) is for the effective longitudinal shear modulus $\overline{G}_{12}$ with $\overline{G}_{12} = G_{12}^s/(R/2)$.

C. Plane-strain bulk modulus

A SWNT subjected to the two-dimensional plane-strain condition of hydrostatic stresses with magnitude σ_K is considered, as shown in Fig. 1(c). Compared with the case of axial tensile loading, the present deformations need to obey the extra plane-strain condition; i.e., the length l of the representative segment of SWNT stays constant.

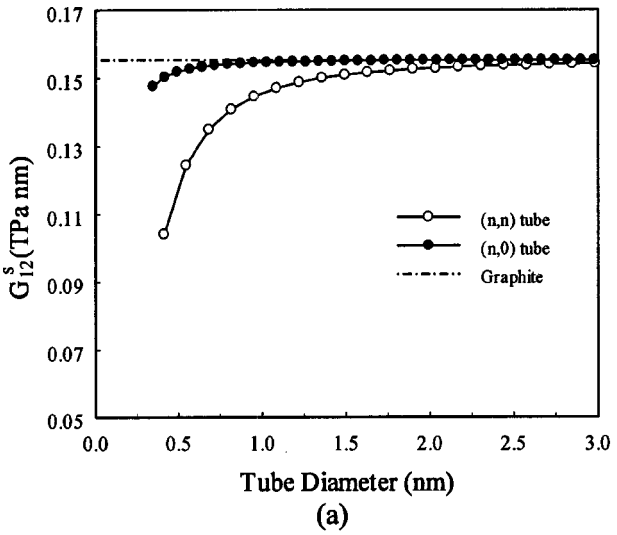

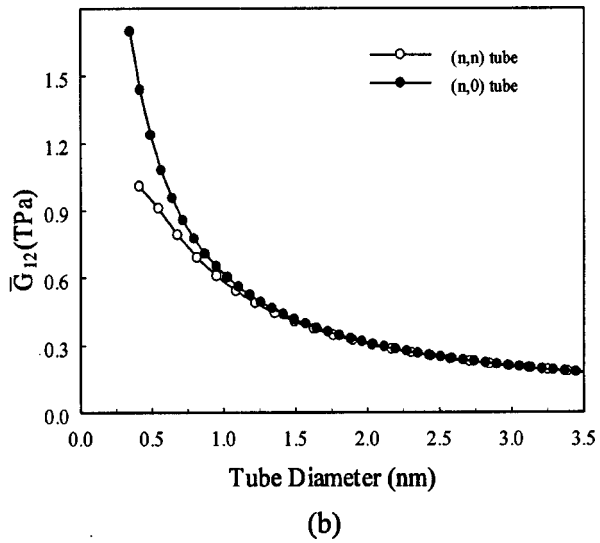

FIG. 6. Variation of the longitudinal shear modulus with the tube diameter: (a) for the surface longitudinal shear modulus and (b) for the effective longitudinal shear modulus.

For a (n,n) armchair SWNT, the plane-strain condition, i.e., $\mathrm{d}l=0$, leads to

$$\mathrm{d}b=-\frac{1}{2}b\cot\frac{\alpha}{2}\mathrm{d}\alpha. \tag{58}$$

The virtual work of the hydrostatic stresses is $W=\sigma_K Sl\mathrm{d}R$, where $\mathrm{d}R$ is the change of the radius of the nanotube. Then, following similar steps to the case of axial tensile loading can lead to

$$\varepsilon_{22}=\frac{2\sqrt{3}\sigma_K R(C_\rho a^2/C_\theta+4\eta_1)}{C_\rho(C_\rho a^2/C_\theta+12\eta_1)}. \tag{59}$$

Using the traditional definition, i.e., $\bar{K}_{23}=\sigma_K/(2\varepsilon_{22})$, for the plane-strain bulk modulus of a cylinder, $\bar{K}_{23}$ of the SWNT can be obtained as

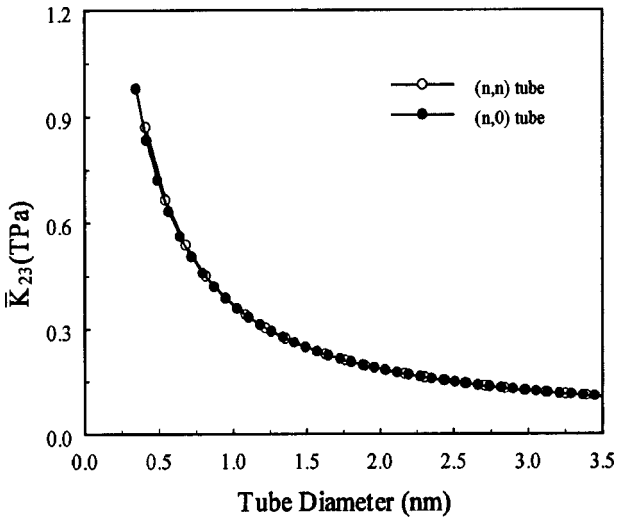

FIG. 7. Variation of the effective plane strain bulk modulus with the tube diameter.

$$\bar{K}_{23}=\frac{\sqrt{3}}{4R}\frac{C_\rho(C_\rho a^2/C_\theta+12\eta_1)}{3C_\rho a^2/C_\theta+12\eta_1}. \tag{60}$$

It is seen that the definition of the plane-strain bulk modulus actually does not involve a thickness like the case of Young's modulus.

For a $(n,0)$ armchair SWNT, the circumferential strain ε_{22} and plane-strain bulk modulus $\bar{K}_{23}$ can be similarly obtained as

$$\varepsilon_{22}=\frac{2\sqrt{3}\sigma_K R(C_\rho a^2/C_\theta+2\eta_2)}{C_\rho(C_\rho a^2/C_\theta+6\eta_2)} \tag{61}$$

and

$$\bar{K}_{23}\frac{\sqrt{3}}{4R}\frac{C_\rho(C_\rho a^2/C_\theta+6\eta_2)}{3C_\rho a^2/C_\theta+6\eta_2}. \tag{62}$$

The variation of the plane-strain bulk modulus $\bar{K}_{23}$ with the diameter is plotted in Fig. 7.

D. In-plane shear modulus

For a SWNT subjected to in-plane pure shear at small strain, its circular cross-sectional perimeter is assumed to bend into an elliptic one like the situation of a thin shell of cylinder as shown in Fig. 8, which is described as

$$\boldsymbol{r}=R(1+\varepsilon_0)\cos\theta\boldsymbol{i}+R(1-\varepsilon_0)\cos\theta\boldsymbol{j},\quad \theta\in[0,2\pi], \tag{63}$$

where the unknown ε_0 characterizes the deformation from the circle with radius R to the ellipse with longer and shorter half-axis $R(1+\varepsilon_0)$ and $R(1-\varepsilon_0)$, and $\boldsymbol{i}$ and $\boldsymbol{j}$ are the unit vectors along the longer and shorter axes. As the deformation is mainly due to the bending, it is assumed that the inversion term is only significant for the total molecular potential energy. The inversion angle variation can be characterized by the rotation angle variation $\mathrm{d}\phi$ for the present case, where ϕ is the rotation angle of the bond a around the axis of the

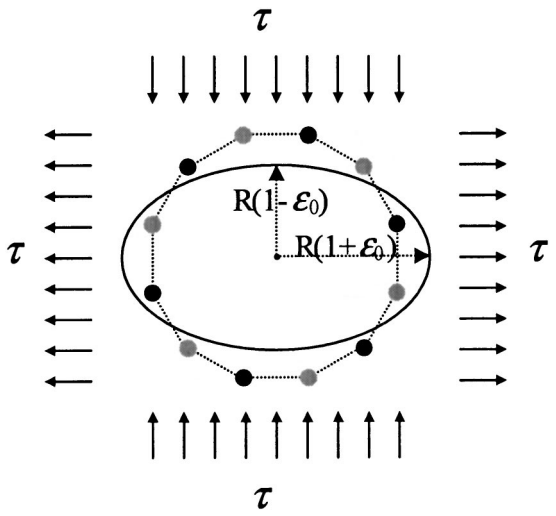

FIG. 8. The assumed deformation mode from a circle to an ellipse of the cross-sectional perimeter of a SWNT subjected to an in-plane pure shear loading condition.

SWNT with the initial values $\phi=\pi/2n$ or π/n for (n,n) or $(n,0)$ nanotube. So the total molecular potential energy, due to inversion can be expressed in terms of the rotation angle variation $\mathrm{d}\phi$ as follows:

$$U=\frac{1}{2}\sum_i C_\phi(\mathrm{d}\phi)^2, \tag{64}$$

where C_ϕ is a modified force constant, which is determined using computational chemistry data.[29,30] The tight-binding calculations[29,30] show that the potential energy per atom of a carbon nanotube rolled up from a graphite sheet is proportional to the squared curvature of the SWNT, which can be rewritten as

$$U_0=\frac{1}{2}C_\kappa\kappa^2, \tag{65}$$

where κ is the curvature of the tube with $\kappa=1/R$, and C_κ is a modified force constant with $C_\kappa=0.0608\ \mathrm{nN\,nm}^3$, which is derived by fitting the computational data.[29,30] For (n,n) and $(n,0)$ nanotubes, C_ϕ can be obtained by correlating Eqs. (64) and (65) as follows:

$$C_\phi=\frac{4C_\kappa}{a^2[1+\cos(\alpha/2)]^2}\ \text{ and }\ C_\phi=\frac{C_\kappa}{a^2\sin(\alpha)^2}. \tag{66}$$

For a (n,n) armchair SWNT, the angle variation $\mathrm{d}\phi$ can be related to the unknown deformation ε_0 as follows:

$$\mathrm{d}\phi=\frac{3}{2}\left(a+b\cos\frac{\alpha}{2}\right)\cos(2\theta)\varepsilon_0\mathrm{d}\kappa, \tag{67}$$

where $\mathrm{d}\kappa$ is the curvature variation when the circular cross-sectional perimeter bends into the elliptic one, which is solved as

$$\mathrm{d}\kappa=3\varepsilon_0\cos(2\theta)/R. \tag{68}$$

Equations (64)–(68) give the potential energy of the atom at the location characterized by angle θ as follows:

$$U_0=\frac{9}{2}C_\kappa\varepsilon_0^2\cos^2(2\theta)/R^2. \tag{69}$$

As the angle θ may vary from 0 to 2π, the average of the potential energy U_0 is only significant, that is,

$$\bar{U}_0=\frac{1}{2\pi}\int_0^{2\pi}U_0\mathrm{d}\theta=\frac{9}{4}C_\kappa\varepsilon_0^2/R^2. \tag{70}$$

So the system potential energy of the representative segment of a SWNT can be given as

$$\Pi=U-W=2n\bar{U}_0-\int_0^{2\pi}\boldsymbol{F}\cdot\mathrm{d}\boldsymbol{u}. \tag{71}$$

Using the external force $\boldsymbol{F}=\sigma_0(\cos\theta\boldsymbol{i}-\sin\theta\boldsymbol{j})$ with $\sigma_0=\tau$ and the corresponding displacement vector $\mathrm{d}\boldsymbol{u}=R\varepsilon_0(\cos\theta\boldsymbol{i}-\sin\theta\boldsymbol{j})$, the total system potential energy becomes

$$\Pi=\frac{9\pi C_\kappa\varepsilon_0^2}{2R[a+b\cos(\alpha/2)]}-2\pi l\sigma_0\varepsilon_0R^2. \tag{72}$$

Then the principle of the minimum potential energy leads to

$$\varepsilon_0=\frac{4\sigma_0}{9C_\kappa}[a+b\cos(\alpha/2)]lR^3. \tag{73}$$

The traditional definition of the in-plane shear modulus, i.e., $\bar{G}_{23}=\sigma_0/(2\varepsilon_0)$, leads to

$$\bar{G}_{23}=\frac{9C_\kappa}{8a(1+\cos(\alpha/2))lR^3}\quad\text{or}\quad\bar{G}_{23}=\frac{\sqrt{3}C_\kappa}{a^2R^3}, \tag{74}$$

where $\alpha=2\pi/3$ and $l=a\sin(\alpha/2)$ have been used to get the reduced form of the formula.

For a $(n,0)$ SWNT, a similar formula can be obtained as follows:

$$\bar{G}_{23}=\frac{9C_\kappa}{8a\sin(\alpha)lR^3}\quad\text{or}\quad\bar{G}_{23}=\frac{\sqrt{3}C_\kappa}{a^2R^3}, \tag{75}$$

where $\alpha=2\pi/3$ and $l=\frac{1}{2}a(1-\cos\alpha)$ have been used for the reduced form of the formula.

As the difference of the potential energies per atom of a carbon nanotube rolled up from a graphite sheet for (n,n) and $(n,0)$ SWNT's with the same diameter is very small,[29,30] the force constants C_κ for (n,n) and $(n,0)$ SWNT's are approximately identical. Thus, the in-plane shear moduli for (n,n) and $(n,0)$ tubes with the same diameter are approximately identical. The variation of the in-plane shear modulus, $\bar{G}_{23}$ with the diameter is plotted in Fig. 9.

III. DISCUSSION AND REMARKS

The closed-form expressions for the local and global deformations of a SWNT, respectively, subjected to axial tension, torsional moment, in-plane biaxial tension, and in-plane pure shear at small strain have been derived using an energy approach in the framework of molecular mechanics. It is

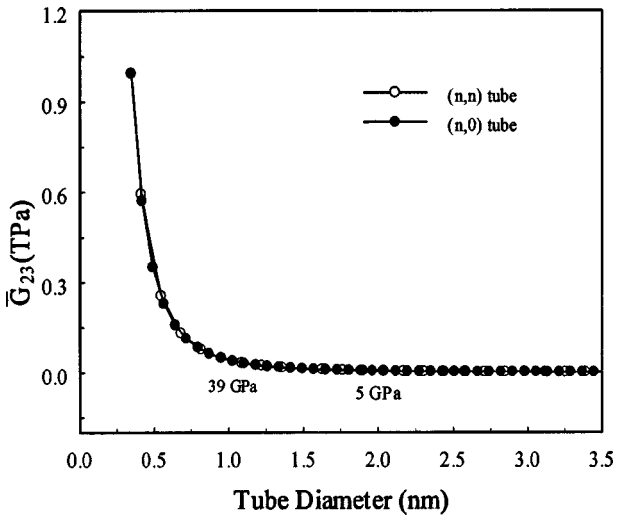

FIG. 9. Variation of the effective in-plane shear modulus with the tube diameter.

noted that the three force constants corresponding to bond stretching, angle variation, and inversion are involved in the present framework of molecular mechanics. The force constants may be obtained by fitting a set of experimental data or the results from a higher level of theories, such as quantum mechanics calculations. In the present calculations, the properties of graphite have been taken as a reference point to get the force constants C_ρ and C_θ, and the force constant C_κ associated with inversion is obtained by fitting the computational chemistry data.[29,30]

The closed-form expressions of the deformations of a SWNT under four loading conditions are independent of the thickness of the SWNT. And the corresponding moduli can be extracted based on various definitions.

For the cases of the axial force and torsional moment, the three definitions for the corresponding longitudinal Young's and shear moduli lead to the three types of Young's and shear moduli, i.e., E_{11}^s and G_{12}^s, E_{11} and G_{12}, and $\bar{E}_{11}$ and $\bar{G}_{12}$ with the relationships $E_{11}=E_{11}^s/t$, $G_{12}=G_{12}^s/t$ and $\bar{E}_{11}=E_{11}^s/(R/2)$, $\bar{G}_{12}=G_{12}^s/(R/2)$. The last types of moduli are also called the effective longitudinal Young's and shear moduli. For the definition of Poisson's ratio, it is seen that the major Poisson's ratio is valid not only for the properties of the thin shell of the SWNT but also for the global SWNT.

TABLE I. The variation of the five effective moduli of a (n,n) armchair SWNT with some typical diameters.

n	$2R$ (nm)	$\bar{E}_{11}$ (TPa)	$\bar{\nu}_{12}$	$\bar{G}_{12}$ (TPa)	$\bar{K}_{23}$ (TPa)	$\bar{G}_{23}$ (TPa)
5	0.682	2.08	0.172	0.791	0.536	0.132
10	1.36	1.06	0.162	0.442	0.271	0.017
15	2.06	0.707	0.161	0.301	0.181	0.005
20	2.71	0.531	0.160	0.227	0.136	0.002
50	6.78	0.213	0.159	0.092	0.055	0.0001

So the Poisson's ratio may also be the effective Poisson's ratio when the SWNT is taken as a solid cylinder. And for the plane strain bulk and in-plane shear moduli, their definitions are just corresponding to the global concepts. So the effective values are only obtained.

The present results for the properties of the thin shell of a SWNT, i.e., E_{11}, ν_{12}, and G_{12}, are basically agreeable with the existing results. And when carbon nanotubes are used as reinforcements of nanocomposites, their global properties, i.e., $\bar{E}_{11}$, $\bar{\nu}_{12}$, $\bar{G}_{12}$, $\bar{K}_{23}$, and $\bar{G}_{23}$, are of concern. The closed-from expressions of the five independent moduli show that the longitudinal Young's and shear moduli, plane-strain bulk modulus, i.e., $\bar{E}_{11}$, $\bar{G}_{12}$, and $\bar{K}_{23}$, explicitly include the factor $1/R$, while the Poisson's ratio $\bar{\nu}_{12}$ does not explicitly include the factor R, and the effective in-plane shear modulus $\bar{G}_{23}$ includes the factor $1/R^3$. So as the tube diameter increases, the effective in-plane shear modulus $\bar{G}_{23}$ abruptly decreases, and the effective Poisson's ratio approaches the value of graphite, as shown in Figs. 9 and 4. Table I lists the variation of the five effective moduli of the (n,n) armchair SWNT with some typical diameters. It is seen that $\bar{E}_{11}$ is approximately the double of $\bar{G}_{12}$ and four times of $\bar{K}_{23}$. The effective Poisson's ratio $\bar{\nu}_{12}$ is approximately a constant, i.e., 0.16, and $\bar{G}_{23}$ is relatively small.

ACKNOWLEDGMENT

This work was supported by NSF, Surface Engineering and Materials Design program, under Grant No. CMS-0305594.

*Corresponding author. Fax: (212) 650-8013. Electronic address: j.li@ccny.cuny.edu

[1] S. Iijima, Nature (London) **354**, 56 (1991).
[2] T. W. Ebbesen and P. M. Ajayan, Nature (London) **358**, 220 (1992).
[3] S. Iijima, C. Brabec, A. Maiti, and J. Bernholc, J. Chem. Phys. **104**, 2089 (1996).
[4] M. R. Falvo, G. J. Clary, R. M. Taylor II, V. Chi, F. P. Brooks, Jr., S. Washburn, and R. Superfine, Nature (London) **389**, 582 (1997).
[5] E. W. Wong, P. E. Sheehan, and C. M. Lieber, Science **277**, 1971 (1997).
[6] O. Lourie and H. D. Wagner, J. Mater. Res. **13**, 2418 (1998).
[7] H. D. Wagner, O. Lourie, Y. Feldman, and R. Tenne, Appl. Phys. Lett. **72**, 188 (1998).
[8] D. A. Walters, L. M. Ericson, M. J. Casavant, J. Liu, D. T. Colbert, K. A. Smith, and R. E. Smalley, Appl. Phys. Lett. **74**, 3803 (1999).
[9] M. F. Yu, B. S. Files, S. Arepalli, and R. S. Ruoff, Phys. Rev. Lett. **84**, 5552 (2000).
[10] M. F. Yu, O. Lourie, M. J. Dyer, K. Moloni, T. F. Kelly, and R. S. Ruoff, Science **287**, 637 (2000).
[11] M. M. J. Treacy, T. W. Ebbesen, and J. M. Gibson, Nature (London) **381**, 678 (1996).

[12] A. Krishnan, E. Dujardin, T. W. Ebbesen, P. N. Yianilos, and M. M. J. Treacy, Phys. Rev. B **58**, 14 013 (1998).
[13] J. P. Salvetat, G. A. D. Briggs, J. M. Bonard, R. R. Bacsa, A. J. Kulik, T. Stöckli, N. A. Burnham, and L. Forró, Phys. Rev. Lett. **82**, 944 (1999).
[14] T. W. Tombler, C. Zhou, J. Kong, H. Dai, L. Liu, C. S. Jayanthi, M. Tang, and S. Y. Wu, Nature (London) **405**, 769 (2000).
[15] J. Muster, M. Burghard, S. Roth, G. S. Duesberg, E. Hernández, and A. Rubio, J. Vac. Sci. Technol. B **16**, 2796 (1998).
[16] Z. W. Pan, S. S. Xie, L. Lu, B. H. Chang, L. F. Sun, W. Y. Zhou, G. Wang, and D. L. Zhang, Appl. Phys. Lett. **74**, 3152 (1999).
[17] D. H. Robertson, D. W. Brenner, and J. W. Mintmire, Phys. Rev. B **45**, 12592 (1992).
[18] G. Overney, W. Zhong, and D. Tomanek, Z. Phys. D: At., Mol. Clusters **27**, 93 (1993).
[19] B. I. Yakobson, C. J. Brabec, and J. Bernholc, Phys. Rev. Lett. **76**, 2511 (1996).
[20] C. F. Cornwell and L. T. Wille, Solid State Commun. **101**, 555 (1997).
[21] J. P. Lu, Phys. Rev. Lett. **79**, 1297 (1997).
[22] T. Halicioglu, Thin Solid Films **312**, 11 (1998).
[23] Y. I. Prylutskyy, S. S. Durov, O. V. Ogloblya, E. V. Buzaneva, and P. Scharff, Comput. Mater. Sci. **17**, 352 (2000).
[24] V. N. Popov, V. E. Van Doren, and M. Balkanski, Phys. Rev. B **59**, 8355 (1999).
[25] P. Zhang, Y. Huang, P. H. Geubelle, P. A. Klein, and K. C. Hwang, Int. J. Solids Struct. **39**, 3893 (2002).
[26] T. Chang and H. Gao, J. Mech. Phys. Solids **51**, 1059 (2003).
[27] Y. Jin and F. G. Yuan, Compos. Sci. Technol. **63**, 1507 (2003).
[28] J. M. Molina, S. S. Savinsky, and N. V. Khokhriakov, J. Chem. Phys. **104**, 4652 (1996).
[29] E. Hernández, C. Goze, P. Bernier, and A. Rubio, Phys. Rev. Lett. **80**, 4502 (1998).
[30] E. Hernández, C. Goze, P. Bernier, and A. Rubio, Appl. Phys. A: Mater. Sci. Process. **68**, 287 (1999).
[31] C. Goze, L. Vaccarini, L. Henrard, P. Bernier, E. Hernandez, and A. Rubio, Synth. Met. **103**, 2500 (1999).
[32] L. Vaccarini, C. Goze, L. Henrard, E. Hernandez, P. Bernier, and A. Rubio, Carbon **38**, 1681 (2000).
[33] D. Sanchez-Portal, E. Artacho, J. M. Soler, A. Rubio, and P. Ordejon, Phys. Rev. B **59**, 12678 (1999).
[34] G. Van Lier, C. Van Alsenoy, V. Van Doren, and P. Geerlings, Chem. Phys. Lett. **326**, 181 (2000).
[35] G. Zhou, W. Duan, and B. Gu, Chem. Phys. Lett. **333**, 344 (2001).
[36] C. Q. Ru, Phys. Rev. B **62**, 9973 (2000).
[37] C. Q. Ru, Phys. Rev. B **62**, 10405 (2000).
[38] C. Q. Ru, J. Mech. Phys. Solids **49**, 1265 (2001).
[39] J. Z. Liu, Q. Zheng, and Q. Jiang, Phys. Rev. Lett. **86**, 4843 (2001).
[40] G. M. Odegard, T. S. Gates, L. M. Nicholson, and K. E. Wise (unpublished).
[41] C. Li and T.-W. Zhou, Int. J. Solids Struct. **40**, 2487 (2003).
[42] A. K. Rappe and C. J. Casewit, *Molecular Mechanics Across Chemistry* (University Science Books, Sausalito, CA, 1997).
[43] L. H. Ye, B. G. Liu, and D. S. Wang, Chin. Phys. Lett. **18**, 1496 (2001).